Microring Resonator Channel Dropping Filters

B. E. Little, S. T. Chu, H. A. Haus, J. Foresi, and J.-P. Laine

***Abstract*—Microring resonators side coupled to signal waveguides provide compact, narrow band, and large free spectral range optical channel dropping filters. Higher order filters with improved passband characteristics and larger out-of-band signal rejection are realized through the coupling of multiple rings. The analysis of these devices is approached by the novel method of coupling of modes in time. The response of filters comprised of an arbitrarily large number of resonators may be written down by inspection, as a continued fraction. This approach simplifies both the analysis and filter synthesis aspects of these devices.**

I. Introduction

CHANNEL dropping filters that access one channel of a wavelength division multiplexed (WDM) signal, and do not disturb the other channels, are useful elements for WDM communications. Resonant filters are attractive candidates for this purpose because they can potentially realize the narrowest linewidth for a given device size. A cascade of coupled resonators can further modify the simple Lorentzian response of a single resonator, yielding desirable higher order filter characteristics. Quarter wave shifted distributed feedback (DFB) resonators, which support standing wave resonant modes, have been proposed for this purpose [1], [2]. A single standing wave resonator side coupled to a signal waveguide can only pick up half of the signal power at resonance. In order to couple out all of the signal power, a second side coupled resonator-reflector is required [2]. Ring or disk resonators support traveling wave resonant modes. By side coupling to a signal bus, Fig. 1, a single ring may completely extract a particular wavelength, and thus offers superior performance compared with that of standing wave resonators. Marcatilli proposed such ring resonator filters in 1969 and analyzed their bending loss [3]. Large radius ring filters have already shown promise [4]–[6]. If the resonators can be made small enough so that the spacing of the resonant frequencies accommodates the set of WDM channels within a communications window, one achieves the goal of dropping one channel by one filter without affecting the other channels. The communications window supported by erbium amplifiers is 30 nm. Rings with a free spectral range (FSR) larger than this would require a radius of 5 μm or less. Fabrication advances have now made it possible to consider structures on the order of a few micrometers [7]–[9]. Here, we consider the details of such microring resonator filters which were proposed in [10]. The emphasis is on filter design using the novel approach of coupling of modes in time, which facilitates both the analysis and filter synthesis aspects of these devices. First, we demonstrate the potential robustness of resonators by calculating the loss limited performance.

The quality or Q of a resonator is a measure of the structures frequency selectivity. The Q is given by the time averaged stored energy per optical cycle, divided by the power coupled or scattered out of the resonator. The Q is limited by radiation loss. A desirable device operating in the wavelength range of 1.3–1.5 μm would have a radiation limited Q on the order of 1500 or greater, in order to achieve a linewidth of 1 nm or less, ($Q \approx \lambda/\Delta\lambda$). One readily calculates that for a typical waveguide of index 3.0, operating in the wavelength range of 1.3–1.5 μm, a loss of 100 dB/cm leads to a radiation limited Q of 5000. A loss of 10 dB/cm results in a radiation Q of 50 000. Thus, the resonator can tolerate moderately large levels in attenuation rate and still provide useful performance. This fact is important, as the large index contrasts required in microresonators leads to large scattering from sidewall imperfections.

Bending loss in smooth, high index contrast rings is negligible. The performance of resonators is thus limited by scattering from sidewall roughness. Such scattering leads to two deleterious effects, that of energy lost to the radiation continuum, and that of scattering into the counterpropagating mode. Radiation loss in disk resonators, and its effect on Q, was analyzed in [11]. Surface roughness induced contradirectional coupling may pose a more serious problem than radiation loss [12]. This arises because the periodic nature of the structure leads to a natural phase-matching between forward and backward waves for any perturbation. Small reflections are thus considerably enhanced. In general, the degree to which scattering limits performance depends on the details of the surface imperfections.

In the following section, we analyze a single ring resonator coupled to a pair of signal waveguides. Here we heuristically develop the description as one of coupling of (energy) modes in time [13]. There is a direct correspondence between circulating power and ring energy. Thus the coupling of modes in time, and the more often encountered coupling of modes in space are made equivalent by relating the energy decay rate to the usual waveguide to waveguide coupling coefficient. In Section III, we consider multiply coupled rings. The solutions to the coupled system may be written down by inspection as a continued fraction. This is in contrast to the usual coupling of modes in space formalism, which can be encumbering even for two coupled rings [5]. The continued fraction representation is

Manuscript received September 19, 1996. This work was supported in part by the National Science Foundation under Grant 9400334-PMR, the National Center for Integrated Photonics Technology under sub-Contract 652693, a Grant from the San Diego Supercomputing Center, and a Natural Sciences and Engineering Research Council of Canada Fellowship.

B. E. Little, H. A. Haus, J. Foresi, and J. P. Laine are with the Department of Electrical Engineering and Computer Science, Massachusetts Institute of Technology, Cambridge, MA 02139.

S. T. Chu is with the Department of Physics and Computing, Wilfred Laurier University, Waterloo, Ont. N2L 3C5, Canada.

Publisher Item Identifier S 0733-8724(97)02701-1.

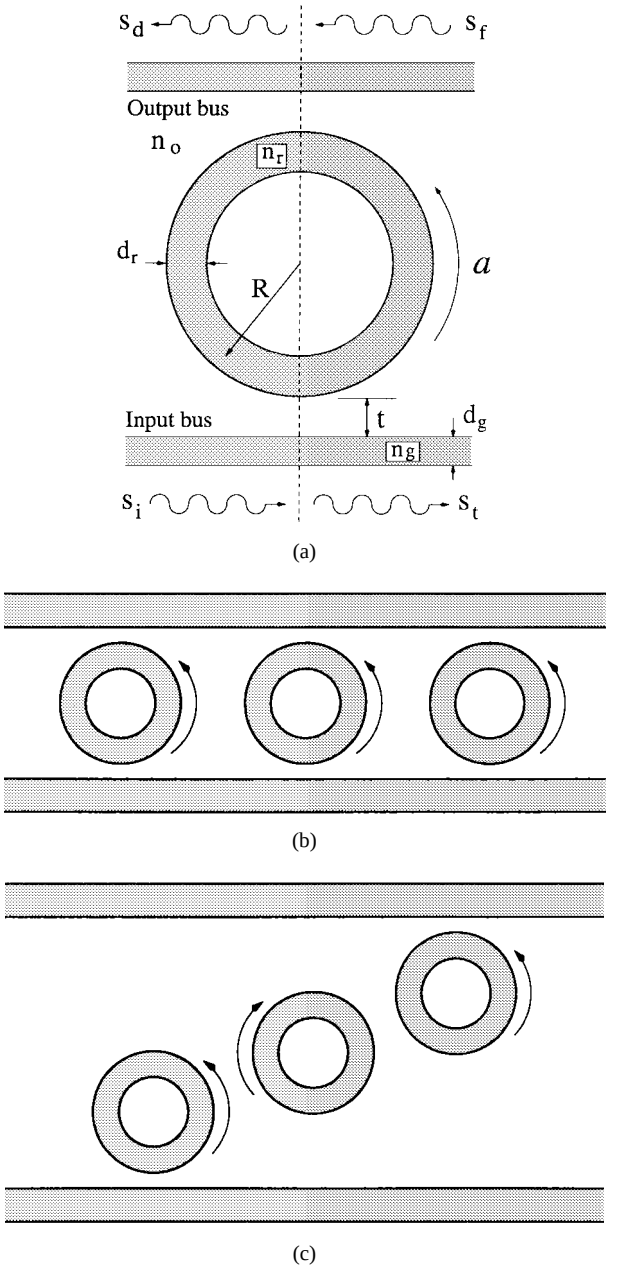

Fig. 1. Microring resonator filters evanescently side coupled to signal waveguides. (a) A single ring of radius R, (measured to the waveguide center). The ring supports a circulating mode with energy amplitude a. The incident wave is s_i, the transmitted wave is s_t, and the filtered or detected wave is s_d. s_f is a feedback wave. (b) and (c) represent higher order filters constructed from a cascade of (b) resonators, (c) or coupled resonators.

useful in the synthesis of higher order filters, which is carried out in Section IV. There, the insertion loss method is employed for filter synthesis and used to construct Maximally, Flat, and Chebyshev responses. The coupled mode results are compared to the more rigorous finite difference time domain (FDTD) [14] simulations throughout. Close correspondence is observed, a result of the weak coupling nature of the problems.

II. Single Ring Resonator

The single ring resonator evanescently side coupled to a pair of signal waveguides is depicted in Fig. 1(a). The ring supports a traveling wave of amplitude $A(t)$, which is normalized such that $|A(t)|^2$ represents the total power flowing through any cross section of the ring waveguide at time t. The ring may also be viewed as a lumped oscillator of energy amplitude $a(t)$, normalized so that $|a(t)|^2$ represents the total energy stored in the ring. Stored energy and power flow in the ring are related through

$$|a(t)|^2 = |A(t)|^2 \frac{2\pi R}{v_g} \tag{1}$$

a relation which will often be used to translate between the "power picture" and "energy picture." R is the ring radius and v_g is the group velocity. The energy in the ring is supplied by the incident wave of amplitude s_i. The filtered output which travels to a detector say, is carried by the detected wave s_d. Power not picked up by the ring is carried away by the transmitted wave s_t. Other rings or devices may feed the signal back to the ring via the feedback wave s_f. The foregoing wave amplitudes are normalized to power.

The ring resonators in Fig. 1 have been analyzed by using the coupling of modes in space, and self-consistent loop equations [4], [5]. Alternatively, here we look at the system as one of coupling of modes in time, treating the ring as a lumped oscillator. The analysis follows closely the derivations in [13]. This oscillator has a resonant frequency of ω_o and an amplitude decay time-constant of $1/\tau$. The decay rate is related to the power leaving the ring, and includes the power coupled externally to the transmitted wave $1/\tau_e$, the power lost due to intrinsic effects such as absorption and surface scattering $1/\tau_\ell$, and power coupled to the output waveguide $1/\tau_d$. Thus, $1/\tau = 1/\tau_e + 1/\tau_d + 1/\tau_\ell$, in this case. From the foregoing energy flow considerations, the time rate of change in ring energy evolves according to

$$\frac{d}{dt}a = \left(j\omega_o - \frac{1}{\tau}\right)a - j\mu s_i \tag{2}$$

where μ is the mutual coupling between the ring and a wave in the signal bus. The equation connecting the incident and transmitted waves is by inspection

$$s_t = s_i - j\mu a. \tag{3}$$

The $-j$ phase factor in front of μ is arbitrarily chosen by the choice of reference planes. Here it was selected so as to have a closer correspondence with the usual coupling of modes is space.

The relation between μ and the external decay rates $1/\tau_e$ and $1/\tau_d$, is determined by power conservation. One considers the case in which the ring is excited to an energy of $|a_o|^2$, there is no detector waveguide $1/\tau_d \to 0$, and no incident signal $s_i = 0$. Then from (2) the ring energy decays as

$$|a(t)|^2 = |a_o|^2 \exp\left(\frac{-2t}{\tau_e}\right) \tag{4}$$

where intrinsic loss has been neglected. We now consider the same scenario in the power picture. The traveling wave of amplitude $A(t)$ in the ring evanescently couples to the

transmitted wave s_t, thus

$$|s_t|^2 = \kappa^2 |A(t)|^2 = \kappa^2 v_g (2\pi R)^{-1} |a(t)|^2 \tag{5}$$

where κ^2 is defined as the fraction of power coupled out of the ring over the interaction region, and use was made of (1). κ is directly related to the usual coupling coefficient of the coupling of modes in space formulation. An analytic expression for κ for slab waveguides is given in the Appendix. Now the power leaving the ring is the time rate of change in energy. Thus, taking the derivative of (4), equating this to (5), and making note of (3) when $s_i = 0$, yields

$$\mu^2 = \kappa^2 v_g (2\pi R)^{-1} = \frac{2}{\tau_e}. \tag{6}$$

μ^2 is seen to be equivalent to the fraction of coupled power κ^2, but is referred to an energy normalization. Throughout, we will refer to κ (and similar coefficients) as the power coupling coefficient, because of its role in coupling two power normalized waves. Equation (6) serves to convert between coupling coefficients with different normalizations, and makes the correspondence between the usual coupling of modes in space and the foregoing coupling of modes in time formulations. A similar relation applies to the coupling of the detector waveguide. The power appearing in the detector waveguide is, by power conservation

$$|s_d|^2 = |s_i|^2 - |s_t|^2 = \frac{2}{\tau_d} |a|^2. \tag{7}$$

III. Transfer Characteristics

The power transfer characteristics are found by considering a steady state incident signal s_i with time dependency $s_i \sim \exp[j\omega t]$. We find from (2)

$$a = \frac{-j\sqrt{\frac{2}{\tau_e}}}{j(\omega - \omega_o) + \frac{1}{\tau}} s_i. \tag{8}$$

When this is introduced into (3) we have

$$s_t = \frac{j(\omega - \omega_o) + \frac{1}{\tau} - \frac{2}{\tau_e}}{j(\omega - \omega_o) + \frac{1}{\tau}} s_i. \tag{9}$$

We can now ask for an adjustment such that all of the signal power is extracted by the resonator at resonance. This is clearly the case when

$$\frac{1}{\tau} = \frac{2}{\tau_e}$$

or

$$\frac{1}{\tau_d} + \frac{1}{\tau_\ell} = \frac{1}{\tau_e}. \tag{10}$$

This finding shows the superiority of a traveling wave resonator over a standing wave resonator. The latter is incapable of transferring the full power without the help of a second resonator-reflector [2]. Even in the presence of loss all power may be extracted, although this requires that the input and detector waveguides are no longer symmetrically coupled to the ring, $\tau_d \neq \tau_e$. When the detector and input waveguides are equally coupled to the ring, the power in the detector is found from (7)

$$|s_d|^2 = \frac{\frac{4}{\tau_e^2}}{(\omega - \omega_o)^2 + \left(\frac{2}{\tau_e} + \frac{1}{\tau_\ell}\right)^2} |s_i|^2. \tag{11}$$

Neglecting loss for the moment, the half-power bandwidth of the detected signal is determined by (11)

$$\Delta\lambda = \frac{2\kappa^2 \lambda_o^2}{(2\pi)^2 R} \frac{v_g}{c} \approx \frac{2\kappa^2 \lambda^2}{(2\pi)^2 R n_e} \tag{12}$$

where we have used $(\omega - \omega_o) \approx \Delta\lambda 2\pi c \lambda_o^{-2}$ and (6). The second form in (12) results when the group velocity v_g is approximated by the phase velocity c/n_e where n_e is the effective index of the ring mode. The bandwidth is proportional to κ^2, the amount of power coupled into the ring over the interaction region.

The quality or Q of the resonator may be calculated by its definition as the time averaged stored energy per optical cycle, divided by the power coupled into the two outgoing waves, (s_d and s_t). The stored energy is given by $|a(t)|^2$. The power coupled into the transmitted wave is given by (5). The power coupled into the detected wave $|s_d|^2$, is identical to (5) when the detector and input waveguides are symmetrically coupled to the ring. Thus

$$Q = \omega_o \frac{|a|^2}{|s_t|^2 + |s_d|^2} = \frac{\omega_o \pi R}{\kappa^2 v_g} \approx \frac{2\pi^2 R n_e}{\lambda_o \kappa^2} \tag{13}$$

where the last expression in (13) results from approximating the group velocity v_g by the phase velocity c/n_e. The Q is controlled by the ring radius and external coupling.

The accuracy of the coupled mode theory is evaluated by comparing the predicted response of a typical microresonator to that of a more rigorous numerical FDTD simulation [14]. Referring to Fig. 1(a), we consider a structure having ring and bus index values of $n_r = n_g = 3.0$, surrounded by air $n_o = 1.0$, and having waveguide widths of $d_r = d_g = 0.2$ μm. The ring has a radius of $R = 1.7$ μm, and the separation of the ring and bus waveguide is $t = 0.2$ μm. The spectral response of the detected power is shown in Fig. 2(a), while Fig. 2(b) shows a snapshot of the electric field intensity in the filter at the resonant wavelength of $\lambda_o = 1.334$ μm. The analytical

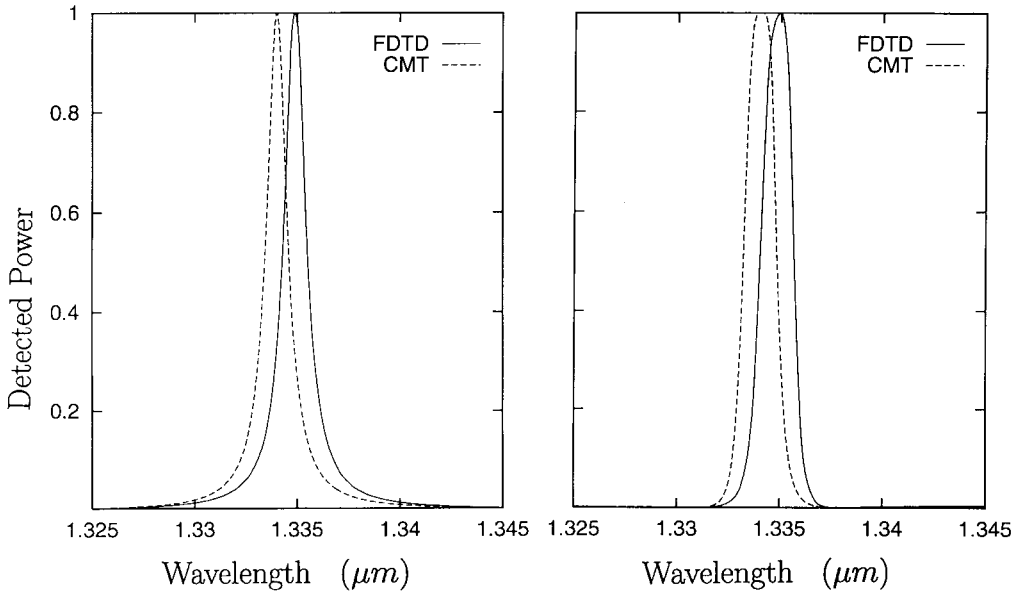

Fig. 3. Higher order filter response of two cascaded rings. (a) Lorentzian response of a single ring compared to (b) the response of two cascaded rings. The solid curves are the results of the numerical FDTD method, while the dashed curves are predictions from the coupled mode theory.

results shown in Fig. 2(a) were generated by the coupling of modes in space [4]–[6], rather than in time, in order to evaluate the response over several resonant peaks. The time domain formulation describes the details of a specific resonance, and its utility will be demonstrated in the following section.

The details of a single resonant peak are shown in Fig. 3, for one and two ring filters. The two ring filter response in Fig. 3(b) is for the cascaded type structure shown in Fig. 1(b) where the reference planes for two identical rings are separated in phase by an odd integer number of π-radians at resonance. The coupled mode theory results (dashed) are slightly shifted from the numerical response (solid). This is due to a few reasons, such as the fact that the numerical structure is discretized and therefore the waveguides deviate in width around a bend. We do not pursue cascaded rings of this type further, since series coupled rings as in Fig. 1(c) offer more attractive features.

IV. Coupled Ring Resonators

By coupling resonators, one may modify the transfer characteristics from that achievable with a single resonator. Thus, for example, the two ring structure of Fig. 4(b) will provide a 12 dB per octave roll-off rate outside of the resonance, and a flattened resonant peak shape. Further, a cascade of dissimilar rings has the important advantage of suppressing the resonances at unwanted wavelengths through the Vernier effect. This can significantly increase the FSR over that of a single ring [4]–[6]. Coupled ring resonators have been analyzed by using the coupling of modes in space formulation. Such an approach can be encumbering, even for two rings [5]. On the other hand, by treating the ring as a lumped resonator oscillating in time, we will show that the response may be evaluated in terms of a continued fraction. This facilitates the synthesis of higher order filter responses.

The time evolution of a single resonator mode was developed in Section II. Consider now the addition of a second resonator as in Fig. 4. As viewed from ring 1, the energy amplitude a_2 in ring 2 may be treated as an additional coupling to a traveling wave. Thus, for resonator 1

$$\frac{d}{dt}a_1 = \left(j\omega_1 - \frac{1}{\tau_e}\right)a_1 - j\mu_1 a_2 - j\mu s_i \qquad (14a)$$

and for resonator 2

$$\frac{d}{dt}a_2 = \left(j\omega_2 - \frac{1}{\tau_d}\right)a_2 - j\mu_1 a_1 \qquad (14b)$$

where μ_1 represents the mutual energy coupling between rings and loss is neglected. μ_1 can be expressed in terms of a power coupling coefficient by power conservation as in Section II, or directly by the following considerations. As viewed from ring 1, the traveling wave in ring 2 of amplitude A_2 plays a similar role to the incident wave s_i, and thus one first considers the additional coupling term to have the form $-j\mu_1' A_2$. Converting to energy normalization by (1), and comparing the term $-j\mu_1 a_2$ in (14a), we arrive at the relation $\mu_1 = \mu_1'\sqrt{v_{g2}(2\pi R_2)^{-1}}$. As μ_1' serves as the coupling between a power normalized wave (A_2) and an energy normalized mode (a_1), the conversion in (6) applies, and thus $\mu_1' = \kappa_1\sqrt{v_{g1}(2\pi R_1)^{-1}}$, where κ_1 is the usual power coupling coefficient. Analytic expressions for κ_1 for slab waveguides are given in the Appendix. Using the foregoing relations we arrive at

$$\mu_1 = \kappa_1\sqrt{v_{g1}v_{g2}(2\pi R_1)^{-1}(2\pi R_2)^{-1}}. \qquad (14c)$$

Following similar derivations, a cascade of N resonators coupled in series is described by the set of coupled differential

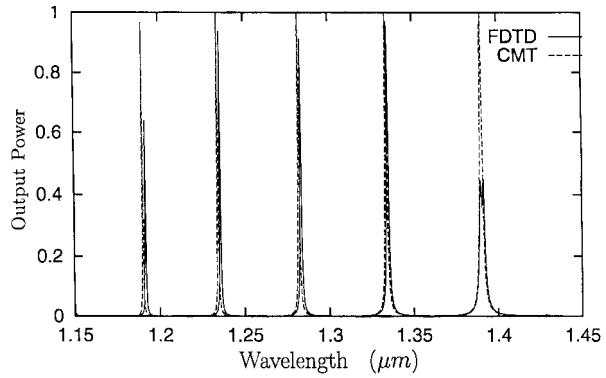

(a)

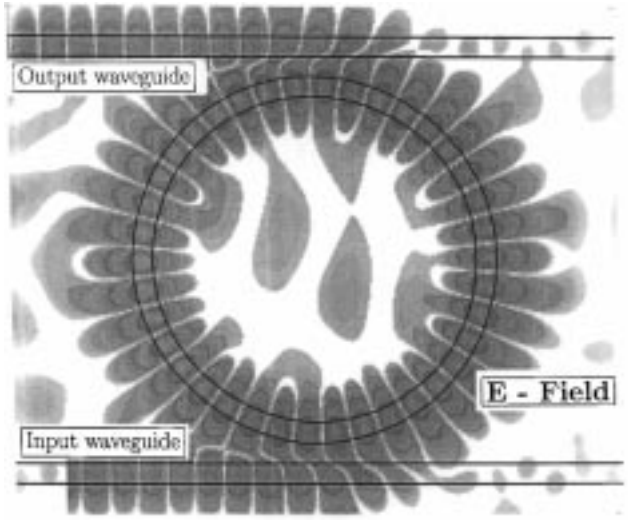

(b)

Fig. 2. Response of a single ring resonator. (a) Wavelength response of the detected port, comparing the coupled mode theory (dashed), to the numerically rigorous FDTD simulation (solid). (b) Instantaneous electric field amplitude in the ring filter near the resonant wavelength $\lambda_o = 1.334\ \mu$m, calculated by the FDTD method. The ring radius is $R = 1.7\ \mu$m, and the core-cladding index contrast is 3:1.

equations

$$\begin{aligned}
\frac{d}{dt}a_N &= \left(j\omega_N - \frac{1}{\tau_d}\right)a_N - j\mu_{N-1}a_{N-1} \\
\frac{d}{dt}a_{N-1} &= j\omega_{N-1}a_{N-1} - j\mu_{N-1}a_N - j\mu_{N-2}a_{N-2} \\
&\cdots \\
\frac{d}{dt}a_2 &= j\omega_2 a_2 - j\mu_2 a_3 - j\mu_1 a_1 \\
\frac{d}{dt}a_1 &= \left(j\omega_1 - \frac{1}{\tau_e}\right)a_1 - j\mu_1 a_2 - j\mu s_i. \qquad (15)
\end{aligned}$$

Each ring oscillates at its own characteristic frequency ω_i, which in the sequel will be set all equal. The terms μ_n represent the resonator couplings

$$\mu_n^2 = \kappa_n^2 \frac{v_{gn}v_{gn+1}}{(2\pi R_n)(2\pi R_{n+1})} \qquad (16a)$$

$$\begin{aligned}
\mu^2 &= \frac{\kappa^2 v_{g_1}}{2\pi R_1} \\
&= \frac{2}{\tau_e} \qquad (16b)
\end{aligned}$$

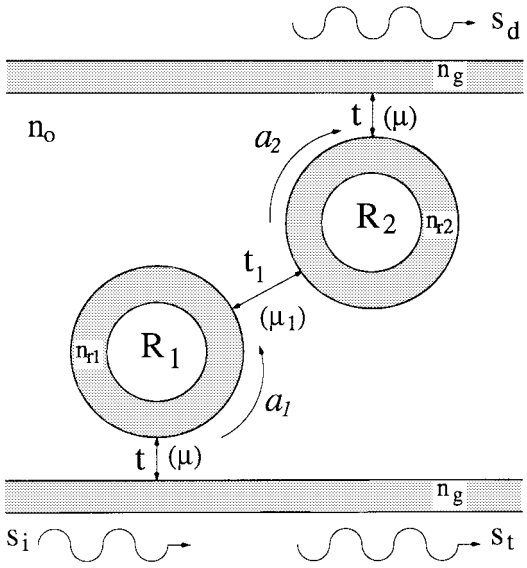

Fig. 4. Series coupled ring resonators, two ring case. The rings support energy amplitudes a_i. μ_i is related to the coupling between rings, while μ is related to the coupling between a ring and the bus. R_i is the radius of ring i measured to the waveguide center.

where v_{gn} is the group velocity of ring n, and R_n is the radius. μ is the coupling between the outer rings and the bus waveguides. It has been assumed that the resonator intrinsic losses are negligible.

The input to the filter may be excited by a monochromatic wave with time dependency $s_i \sim \exp[j\omega t]$. The time dependency of all the resonators must follow suit, $a_j(t) = a_j \exp[j\omega t]$. With this substitution in (15), the response of resonator one can be arranged into the continued fraction

$$a_1 = \cfrac{-j\mu s_i}{j\Delta\omega_1 + \cfrac{1}{\tau_e} + \cfrac{\mu_1^2}{j\Delta\omega_2 + \cfrac{\mu_2^2}{j\Delta\omega_3 \cdots + \cfrac{\mu_{N-1}^2}{j\Delta\omega_N + \cfrac{1}{\tau_d}}}}} \qquad (17)$$

with the definition for frequency deviation

$$\Delta\omega_j = \omega - \omega_j. \qquad (18)$$

The relation between incident and outgoing waves (3) and (7) remains unchanged. Expression (17) allows one to construct the filter solution for large numbers of rings by inspection. In the following, we show how the selection of coupling ratios between rings μ_j, relative to that of the coupling to the signal bus μ, yields some standard electrical filter performances.

V. Filter Synthesis

Ring resonators are attractive because they offer the possibility of realizing desirable filter characteristics in a compact size. Various filter functions are realized through the appropriate selection of ring coupling coefficients μ_n in (17). In close analogy with electrical filter design, one is manipulating the pole locations of each resonator. Indeed, we proceed to

analyze the system of rings with techniques borrowed from circuit design [15], [16]. Recently, Orta *et al.* [17] have shown how to approach the filter synthesis problem of multiple rings from the coupling of modes in space formalism. Although in principle identical in the limit of weak coupling, here we follow the analysis as one of coupling of modes in time. We focus on achieving two types of response, maximally flat and Chebyshev.

The insertion loss method is particularly well suited for synthesizing rational function responses [15]. In the insertion loss method, the response is defined to be the power loss ratio, which is the ratio of total incident power to power present at the detected port. The power loss ratio has the form

$$P_{LR}(\Delta\omega) \equiv \frac{|s_i|^2}{|s_d|^2} = 1 + P_N(\Delta\omega^2). \tag{19}$$

For the response governed by the continued fraction in (17), and the detected power in (7), P_{LR} is a polynomial in $\Delta\omega^2$, emphasized by the polynomial function of order N, $P_N(\Delta\omega^2)$. For a maximally flat response, the coefficients of all orders of $\Delta\omega^2$ except for the highest, must vanish. This implies that for a cascade of N resonators

$$P_N(\Delta\omega^2) = A_N \Delta\omega^{2N} \tag{20}$$

where A_N is some constant related to the roll-off at the band edges. A Chebyshev response requires

$$P_N(\Delta\omega^2) = k^2 T_N^2\left(\frac{\Delta\omega}{\Delta\omega_c}\right) \tag{21}$$

where T_N is the Chebyshev polynomial of order N, and k^2 measures the magnitude of the ripple below unity in the passband. $\Delta\omega_c$ is the bandwidth at which the response drops k^2 from unity at the band edges. In what follows, it is not necessary that $\Delta\omega_c$ be evaluated.

Filter synthesis for maximally flat and Chebyshev responses have been considered, and the results are summarized in Table I for from two to six rings. This table gives the mutual coupling coefficients between rings μ_i, relative to the coupling of the outer rings to the signal waveguides μ. Equation (16) may be used to convert μ and μ_n to power coupling coefficients if necessary. To demonstrate the synthesis approach, we consider the details of the analysis for two coupled rings. The power loss ratio is first written in polynomial form using (7) and (17) in (19)

$$P_{LR} = 1 + \frac{1}{\mu^4\mu_1^2}\left[\Delta\omega^4 + \left(\frac{\mu^4}{2} - 2\mu_1^2\right)\Delta\omega^2 + \left(\mu_1^2 - \frac{\mu^4}{4}\right)^2\right]. \tag{22}$$

Maximally flat response is achieved when μ_1^2 is selected to make the constant and quadratic terms in the bracket vanish. Thus

$$\mu_1 = \frac{\mu^2}{2} \tag{23}$$

TABLE I

N	Maximally Flat	Chebyshev
2	$\mu_1^2 = 0.250\mu^4$	$\mu_1^2 = 0.250\mu^4(1+2k)$
3	$\mu_1^2 = \mu_2^2 = 0.125\mu^4$	$\mu_1^2 = \mu_2^2 = 0.125\mu^4(1+1.5k^{(2/3)})$
4	$\mu_1^2 = \mu_3^2 = 0.100\mu^4$ $\mu_2^2 = 0.040\mu^4$	
5	$\mu_1^2 = \mu_4^2 = 0.0955\mu^4$ $\mu_2^2 = \mu_3^2 = 0.0295\mu^4$	
6	$\mu_1^2 = \mu_5^2 = 0.0915\mu^4$ $\mu_2^2 = \mu_4^2 = 0.0245\mu^4$ $\mu_3^2 = 0.0179\mu^4$	

which is the first entry in Table I. If the rings are fabricated from identical waveguides, but have different radii, R_1 and R_2, this reduces to the selection of power coupling ratios as,

$$\kappa_1 = \frac{1}{2}\sqrt{\frac{R_2}{R_1}}\,\kappa^2. \tag{24}$$

We now consider some examples of multiple coupled ring filters. Fig. 5 compares the passband characteristics of filters comprised of one, two, and three coupled rings. The following selection of parameters were chosen to obtain maximally flat response: the radius of all rings are $R_i = 1.7$ μm; the index values of all rings and the bus waveguides are $n_{ri} = n_{g1} = n_{g2} = 3.0$; the cladding index is $n_o = 1.0$; the widths of all the rings and bus waveguides are $d_{ri} = d_{g1} = d_{g2} = 0.2$ μm; the distance between the outer rings and bus waveguides are $t = 0.2$ μm; for the two ring filter $t_1 = 0.36$ μm; for the three ring filter $t_1 = t_2 = 0.39$ μm. It is evident in Fig. 5(a) and (b) that as the number of rings increases, the filter response becomes more "box like."

A numerically rigorous FDTD [14] simulation of the two ring filter is shown in Fig. 6. Fig. 6(b) shows the average electric field intensity in the filter at the wavelength of $\lambda_o = 1.334$ μm. Fig. 6(a) compares the passband characteristics as predicted by the CMT and FDTD methods. The results show a relative shift in the locations of the characteristics, a result that the FDTD structure is discretized, and due to possible higher order bending effects which change the ring waveguide propagation constant.

VI. Summary

Compact filters composed of ring resonators have been analytically analyzed by the method of coupling of modes in time. In this method, the rings are considered as oscillators in time. The approach leads to solutions of the multiple ring problem which can be written down by inspection, as a continued fraction. The analysis and filter synthesis aspects are facilitated by this analytic form. Multiple coupled rings can improve the filter performance over that of a single resonator by providing larger of-of-band signal rejection, and a flat passband. The insertion loss method of electric filter design is used to obtain the appropriate coupling values between rings in order to achieve maximally flat response. Comparisons of the analytic theory with that of more rigorous numerical

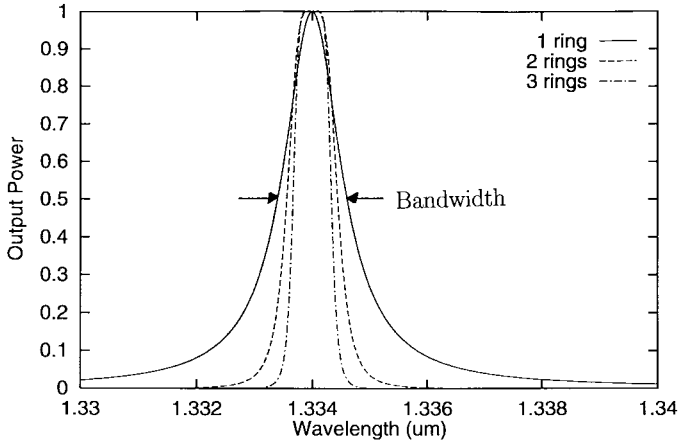

(a)

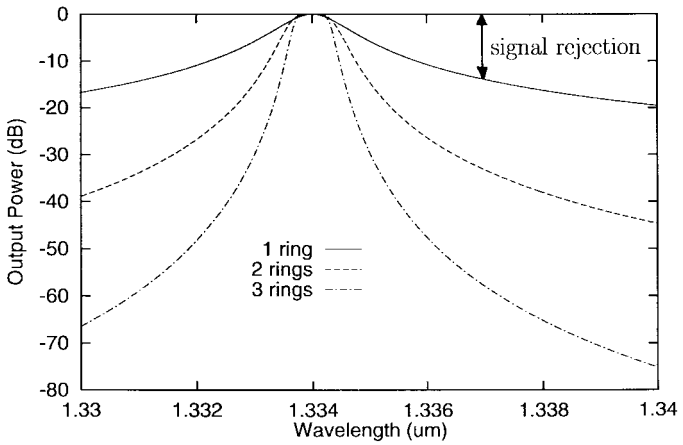

(b)

Fig. 5. A comparison of the passband characteristics of filters composed of one, two, and three coupled rings. The parameters of each filter were selected with the help of Table I, so as to obtain a Maximally Flat response. A more "box-like" response is the result of utilizing additional rings.

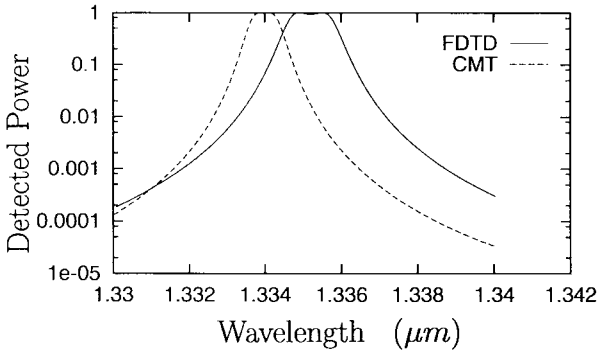

(a)

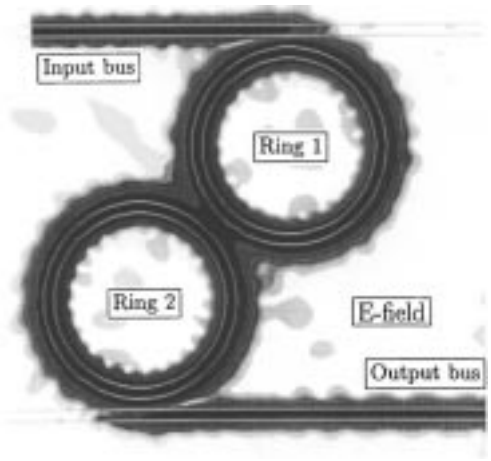

(b)

Fig. 6. A comparison of CMT and numerically rigorous FDTD predictions for the two-ring filter. (a) Passband characteristics. The CMT and FDTD characteristics are relatively displaced (by about 1% of the carrier wavelength) due to the nature of the discretized FDTD filter, as well as possible higher order bending effect which modify the ring waveguide propagation constant. (b) The average electric field magnitude in the device at the resonant wavelength of 1.334 μm.

methods show close correspondence, a consequence of the weak coupling between modes. A relative shift of the response characteristics is observed between analytic and numerical solutions. This shift may be due to the discretized nature of the numerically simulated structure or possibly due to higher order effects of the curved ring waveguide.

APPENDIX

Two rings, or a ring and a signal bus, exchange power when they are in close proximity. Because the rings are curved, the interaction length is short, and only a small fraction of power is exchanged. As indicated by (13), a small coupling κ is desirable to achieve a large Q. Since only a small fraction of power is exchanged, the coupled amplitudes do not change appreciably over the interaction region. The coupling is considered lumped at the dashed reference plane shown in Fig. 1. In this Appendix, we give analytic formulas for κ for slab waveguide structures, following standard coupled mode theory treatment such as in [13] and [18].

The index profile of two coupled waves is shown in Fig. 7. The widths of waveguides one and two are $2w_1$ and $2w_2$, their refractive indexes are n_1 and n_2, and are embedded in a surrounding cladding of index n_o. The waveguide centers are separated by the distance $2s$. Both waveguides are assumed to be rings with radius R_1 and R_2, measured to the waveguide centers. If one of the waveguides is a straight signal bus, then $R_i \to \infty$ in the following formulas.

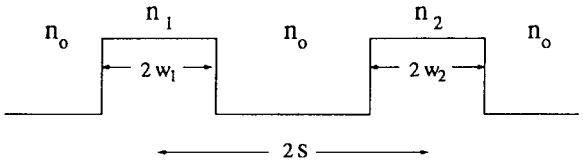

Fig. 7. Geometry and index profile of two coupled waveguides.

From [18], the instantaneous coupling strength is evaluated by the overlap integral

$$\kappa[s(z)] = \frac{\epsilon_o \omega}{4} \int_{\infty}^{\infty} (n_1^2 - n_o^2)\mathbf{e}_1(x)\mathbf{e}_2^*(x)\,dx. \qquad \text{(A1)}$$

$\mathbf{e}_1(x)$ and $\mathbf{e}_2(x)$ are the power normalized modal fields in individual waveguides 1 and 2, ϵ_o is the permittivity of free space, and ω is the circular frequency. The net coupled amplitude is proportional to the integral of $\kappa[s(z)]$ over the

interaction region, weighted by the phase mismatch of the waveguide modes

$$\kappa = \int_{\infty}^{\infty} \kappa[s(z)] e^{-j\Delta\beta z}\, dz. \tag{A2}$$

The phase mismatch is $\Delta\beta = \beta_1 - \beta_2$ where β_i is the propagation constant of waveguide i. The coupling $\kappa(s)$ depends exponentially on guide separation s, and is thus only nonnegligible in the region of smallest separation. We treat the curvature as parabolic

$$\begin{aligned} s &= s_o + \gamma z^2 \\ \gamma &= \frac{1}{2R} \\ R &= \frac{R_1 R_2}{R_1 + R_2}. \end{aligned}$$

R is the effective radius of curvature and $2s_o$ is the smallest separation between the waveguides, center to center. Evaluating (A1) and (A2) with the algebraic details omitted results in

$$\begin{aligned} \kappa = {} & \frac{\omega\epsilon_o \cos(k_{x2} w_2)}{2\sqrt{P_1 P_2}(k_{x1}^2 + \alpha_2^2)} (n_1^2 - n_o^2) \\ & \times \sqrt{\frac{\pi R}{\alpha_2}} \exp[\alpha_2(w_2 - 2s_o)] \\ & \times [\alpha_2 \cos(k_{x1} w_1) \sinh(\alpha_2 w_1) \\ & + k_{x1} \sin(k_{x1} w_1) \cosh(\alpha_2 w_1)] \end{aligned} \tag{A3}$$

P_i is the mode power, α_i is the decay constant in the cladding, and k_{xi} is the transverse propagation constant in the core, all of guide i

$$\begin{aligned} P_i &= \frac{\beta_i}{2\omega\mu_o}\left(w_i + \frac{1}{\alpha_i}\right) \\ \alpha_i &= \sqrt{\beta_i^2 - n_o^2 k^2} \\ k_{xi} &= \sqrt{n_i^2 k^2 - \beta_i^2} \end{aligned} \tag{A4}$$

where k is the free space wave vector.

REFERENCES

[1] H. A. Haus and R. V. Schmidt, "Transmission response of cascaded gratings," *IEEE Trans. Sonics Ultrason.*, vol. SU-24, pp. 94–101, 1977.

[2] H. A. Haus and Y. Lai, "Theory of cascaded quarter wave shifted distributed feedback resonators," *J. Quantum Electron.*, vol. 28, pp. 205–213, 1992.

[3] E. A. J. Marcatilli, "Bends in optical dielectric waveguides," *B.S.T.J.*, vol. 48, pp. 2103–2132, 1969.

[4] P. Urquhart, "Compound optical-fiber-based resonators," *J. Opt. Soc. Amer. A*, vol. 5, pp. 803–812, 1988.

[5] K. Oda, N. Tokato, and H. Toba, "A wide-FSR waveguide double-ring resonator for optical FDM transmission systems," *J. Lightwave Technol.*, vol. 9, pp. 728–736, 1991.

[6] S. Suzuki, K. Oda, and Y. Hibino, "Integrated-optic double-ring resonator with a wide free spectral range of 100 GHz," *J. Lightwave Technol.*, vol. 13, pp. 1766–1771, 19.

[7] Y. Yamamoto and R. E. Slusher, "Optical processes in microcavities," *Phys. Today*, pp. 66–73, June 1993.

[8] Z. Zhang, D. Chu, S. Wu, S. Ho, W. Bi, C. Tu, and R. Tiberio, "Photonic-wire laser," *Phys. Rev. Lett.*, vol. 75, pp. 2678–2681, 1995.

[9] S. L. McCall, A. F. J. Levi, R. E. Slusher, S. J. Pearton, and R. A. Logan, "Whispering-gallery mode microdisk lasers," *Appl. Phys. Lett.*, vol. 60, pp. 289–291, 1992.

[10] B. E. Little, S. T. Chu, and H. A. Haus, in *LEOS 8th Annu. Meeting*, Inst. Elec. Electron. Eng., NY, 1995, paper WDM 2.3.

[11] B. E. Little and S. T. Chu, "Estimating surface roughness loss and output coupling in microdisk resonators," *Opt. Lett.*, vol. 21, pp. 1390–1392, 1996.

[12] B. E. Little, J.-P. Laine, and S. T. Chu, "Surface-roughness-induced contradirectional coupling in ring and disk resonators," *Opt. Lett.*, vol. 22, pp. 4–6, 1997.

[13] H. A. Haus, *Waves and Fields in Optoelectronics, Chapter*. Englewood Cliffs, NJ: Prentice Hall, 1984.

[14] S. T. Chu and S. K. Chaudhuri, "A finite-difference time-domain method for the design and analysis of guided-wave optical structures," *J. Lightwave Technol.*, vol. 7, pp. 2033–2038, 1989.

[15] R. Collins, *Foundations for Microwave Engineering*. New York: McGraw-Hill, 1966.

[16] A. I. Zverev, *Handbook of Filter Synthesis*. New York: Wiley, 1967.

[17] R. Orta, P. Savi, R. Tascone, and D. Trinchero, "Synthesis of multiple-ring-resonator filters for optical systems," *IEEE Photon. Technol. Lett.*, vol. 7, pp. 1447–1449, 1995.

[18] H. A. Haus, W. P. Haung, S. Kawakami, and N. A. Whitaker, "Coupled-mode theory of optical waveguides," *J. Lightwave Technol.*, vol. LT-5, pp. 16–23, 1987.

B. E. Little, photograph and biography not available at the time of publication.

S. T. Chu, photograph and biography not available at the time of publication.

H. A. Haus, photograph and biography not available at the time of publication.

J. Foresi, photograph and biography not available at the time of publication.

J.-P. Laine, photograph and biography not available at the time of publication.